SOUND SOURCE LOCALIZATION EMPLOYING POLAR DIRECTIVITY PATTERNS OF BIDIRECTIONAL MICROPHONES

Vijay Varada, The University of Toledo; Hong Wang, The University of Toledo; Vijay Devabhaktuni, The University of Toledo

Abstract

This paper introduces a novel-sound-source localization technique using an array of bidirectional microphones. Specifically, the proposed technique exploits the polar directivity pattern of three bidirectional microphones to provide complete 360° localization coverage. The feasibility of this approach has been tested through both simulations and experiments. An algorithm was developed specifically for the proposed method. This technique reduces the total number of microphones required to provide similar coverage to the recently introduced unidirectional microphone-based-localization technique. At the same time, the overall spatial displacement requirements for the sensors were significantly reduced compared to the existing time-domain and phased-array methods.

Introduction

Sound-source localization (SSL) may be defined as identifying the location of a detected sound source. Sound-source localization techniques are usually passive with broad applications. For example, in warfare, SSL is used to enhance the patrol capability of troops [1], [2]. In conference meetings, SSL is used to direct and zoom cameras towards the speaker for a better viewing experience. In teleconferencing, it helps by allowing the network bandwidth to be more efficient [3], [4]. Sound-source localization may also be very important in humanoid robots and hearing aids. Finally, SSL can be employed in nocturnal activities such as night-hunting.

Due to its widespread applications, SSL has been an interesting topic for researchers over the past two decades, and various SSL techniques have appeared in literature [5-9]. In general, these techniques can be classified into three main categories, namely, beam-forming, time-delay, and spectral analysis [10-13]. In beam-forming, the microphone signal is steered in all possible directions to maximize the output [14], [15]. In time-delay methods, the time-of-arrival of the sound signal on different sensors is used for localization. In spectral analysis, spatial-spectral correlation among the received signals (usually narrowband) is used for source localization. Hybrid methods that combine beam-forming and time-delay have also been proposed [10], [16], [17]. These techniques, however, are limited by the very large spatial-displacement requirements of the sensor, and, therefore, may not be practical in confined environments. Recently, a new approach exploiting the polar directivity pattern (PDP) of unidirectional microphones has been proposed [1]. This approach allows reduced sensor spacing compared to the prevalent methods. However, it provides limited SSL coverage in the plane of the microphone sensor array.

This paper introduces a new SSL method based on the use of bidirectional microphones. The proposed method provides complete 360° SSL coverage, while maintaining the reduced spatial-displacement requirements for the sensors. The unidirectional microphone-based SSL technique is discussed in Section 2, followed by the proposed approach in Section 3. Section 4 discusses the simulation results, followed by Sections 5 and 6, which present the experimental setup and results. Lastly, the conclusions are given in Section 7.

Prevalent SSL Technique Based on PDPs of Unidirectional Microphones

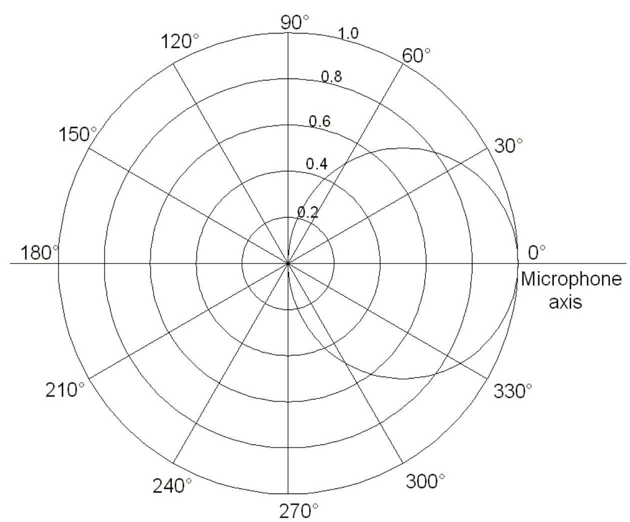

Figure 1. General polar directivity pattern of a first-order unidirectional microphone

The sensitivity/response of directional microphones has a strong dependence on the incidence angle of the sound signal described by equation (1) as

$$N = P + G * \cos\theta , \qquad (1)$$

where N is the sensitivity of the microphone, P is the pressure on the diaphragm of the microphone caused by the incident sound wave, and θ is the angle of incidence of the acoustic signal. G is the gradient and is defined as the difference of pressure on either side of the diaphragm [18]. The general polar-directivity pattern of a first-order unidirectional microphone can be plotted as in Figure 1. As can be seen, the microphone gives the maximum output for $\theta = 0°$, while for $90° < \theta < 270°$, the microphone output is zero.

The normalized output (N) of a directional microphone provides the angle of incidence of a detected signal in the PDP. Each normalized value can be geometrically represented as a circle of radius N_i (Figure 1). This circle intersects the PDP of the microphone giving rise to two angles for each normalized output. In the unidirectional microphone-based SSL technique [1], three microphones are arranged in a circular array. Two lines, corresponding to each normalized microphone output, are drawn from each microphone. Triangulation is then used to localize the sound source. However, this technique does not provide 360° coverage.

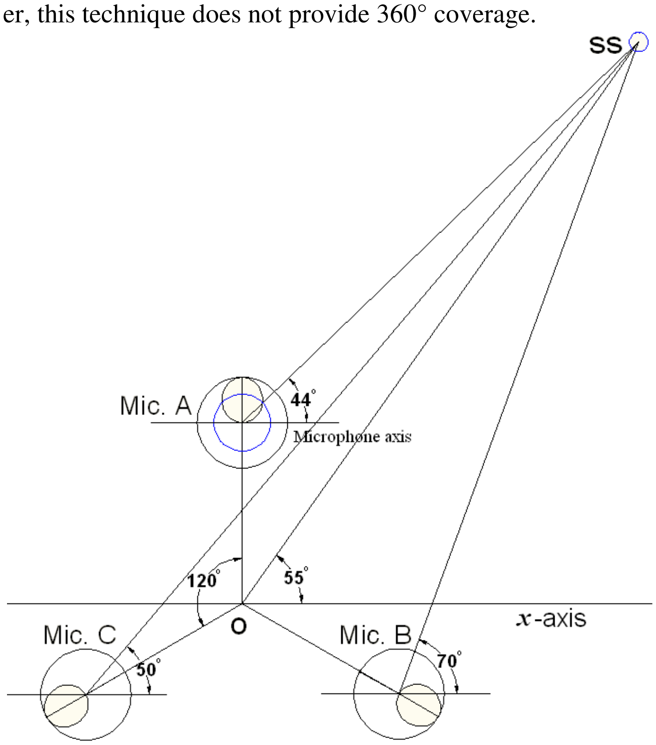

Figure 2. Localization using unidirectional microphones oriented at angles 90°/330°/210°

This disadvantage can be illustrated using the example shown in Figure 2. Here, three unidirectional microphones (labeled A, B, and C) are spaced equally on a circular path such that their axes are directed to 90°, 330°, and 210° with respect to the x-axis. A sound signal originating from a sound source (SS) located at an angle of 55° with respect to origin O will arrive at angles 44°, 70° and 50° to the microphones A, B, and C, respectively. Using these values, one can find θ_A, θ_B and θ_C, which are the angles of the sound signal with respect to the microphone axes as shown in Figure 2. By using these angles, one can get the normalized values. As can be deduced from Figure 2, microphone A has some output, but microphones B and C produce zero output, i.e. they do not pick-up any signal. This means that localization cannot be performed for this particular source location, which can be referred to as a blind spot. To reduce the number of such blind spots, it is recommended to use more than three microphones in the array [1].

Proposed Approach

Bidirectional microphones have double 'listening capacity' and provide more information than unidirectional microphones [18]. This paper proposes using three bidirectional microphones, which have two lobes in their PDPs to remove the blind spots. Such an approach could make the system more robust. As will be shown, the proposed approach provides complete 360° localization with no blind spots. Substituting $P = 0$ and $G = 1$ for the bidirectional microphones in equation (1) [18], the polar equation becomes

$$N = \cos\theta . \qquad (2)$$

The corresponding bidirectional PDP is plotted in Figure 3.

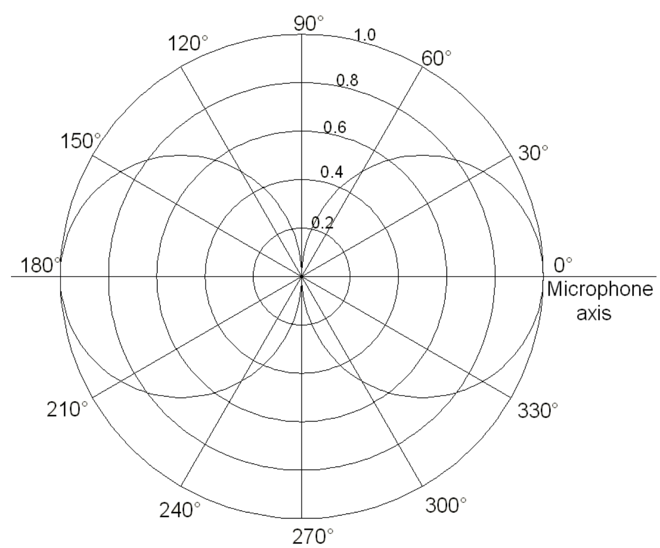

Figure 3. General PDP of a bidirectional microphone

For illustration of the proposed technique, consider Figure 4 showing three bidirectional microphones A, B, and C. Once again, the microphones are equally spaced and are located in a circular arrangement at 90°, 330°, and 210°, respectively.

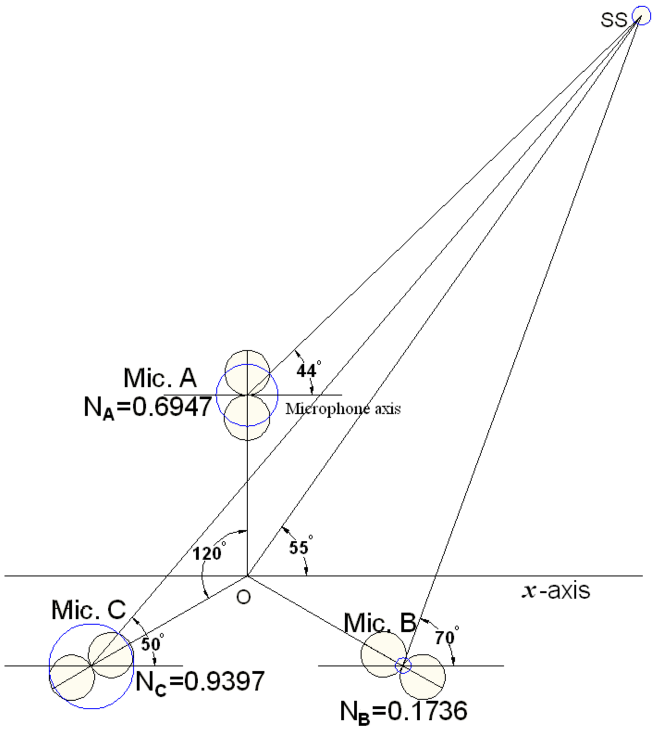

Figure 4. Localization using bidirectional microphones oriented circularly at angles 90°/330°/210°

Let normalized outputs from microphones A, B, and C be

$$N_A = \cos\theta_A, \tag{3}$$

$$N_B = \cos\theta_B, \tag{4}$$

$$N_C = \cos\theta_C, \tag{5}$$

where θ_A, θ_B and θ_C are angles with respect to the microphone axes. As can be inferred from Figure 3, corresponding to each normalized value, N_i (i = A, B, or C), there are four angles in a bidirectional PDP. For each normalized output, four straight lines can be extended from the center of each microphone. Since the lobes are symmetrical, these lines connect at the microphone centers such that there are only two lines crossing the microphone center. The intersection of these lines leads to the localization of sound sources using the algorithm of Figure 5. The corresponding pseudo-code is presented in Table 1.

Simulation Results

For validation of the proposed approach, consider Figure 4, where three bidirectional microphones are arranged in a circular array. Each microphone is located at a distance of 4 units from the origin O, with their centers at (0, 4), (3.4641, -2.0), and (-3.4641, -2.0), respectively. The sound source, SS, is located at (8.7650, 12.4053). By using equation (2), the normalized outputs (N_A, N_B, and N_C) from the microphones are 0.6947, 0.1736, and 0.9397. Corresponding to these normalized values, the potential incidence angles with respect to of the x-axis are, 44° and 136° at microphone A, 50° and 70° at microphone B, and 10° and 50° at microphone C.

The algorithm in Figure 5 was employed to trace the lines along the potential angles of incidence and to calculate the intersection points. Using all possible combinations, the triangle with the smallest area was determined. In practice, the instrument noise and acoustic propagation variations lead to triangles with finite areas.

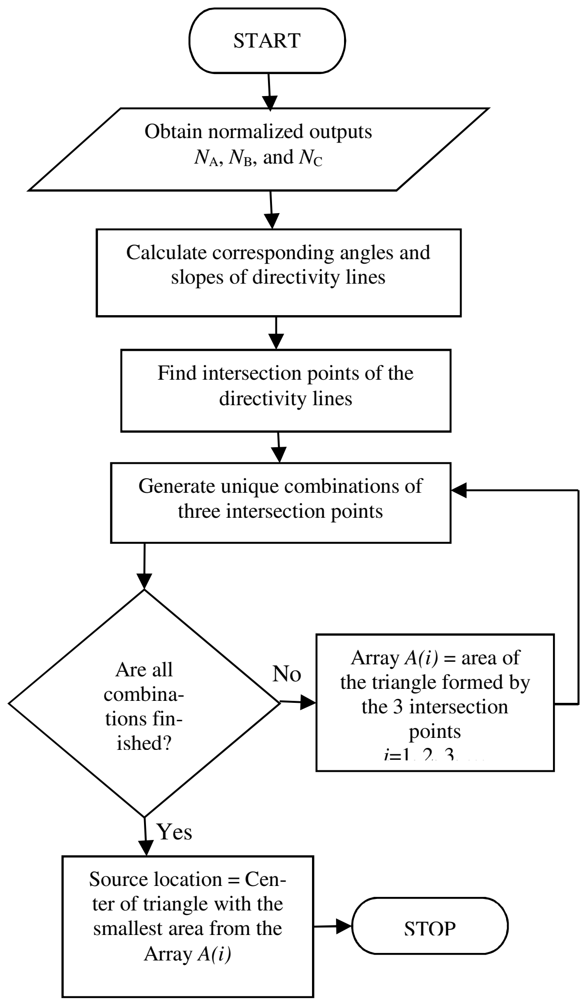

Figure 5. Flowchart of the proposed algorithm

However, since this simulation did not account for these imperfections, the lines intersected exactly at (8.7650, 12.4053) which is, in fact, the location of the SS. A plot depicting the directivity lines (A_1, A_2; B_1, B_2, and C_1, C_2) and their intersections is shown in Figure 6.

To check for the coverage of the proposed technique, the simulation was repeated with a 360° sweep of the SS placed at a distance of 12 units from the origin *O*. The results plotted in Figure 7 show complete 360° coverage with no null points.

Table 1: Pseudo-code of the proposed approach

Step 1: Let the normalized outputs of the microphones be N_A, N_B, and N_C. Find the angle of incidence θ with respect to the microphone axis using

$$N_i = \cos\theta_i,$$

$$\text{where } i \in [A, B, C].$$

Step 2: Calculate the angles of the directivity lines α_A, β_A, α_B, β_B, and α_C, β_C using

$$\alpha_i = \theta_i + \phi_i \text{ and } \beta_i = \theta_i - \phi_i,$$

$$\text{where } i \in [A, B, C]$$

and ϕ_i is the orientation of the microphone.

Step 3: Draw two lines from each microphone center:

$$\text{Line 1: } (y - y_i) = \tan\alpha_i (x - x_i),$$

$$\text{Line 2: } (y - y_i) = \tan\beta_i (x - x_i),$$

$$\text{where } i \in [A, B, C].$$

Step 4: Solve pairs of these lines to obtain an array of intersection points *P*.

Step 5: The center of the smallest triangle formed by any three points$\in P$ is the source location.

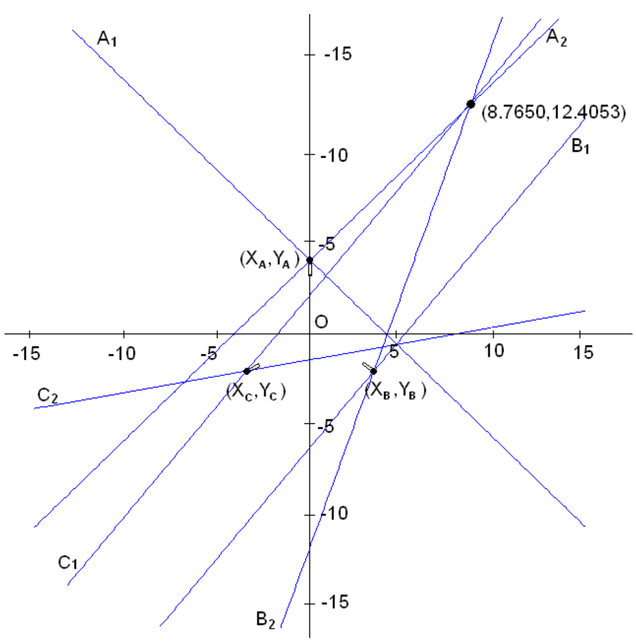

Figure 6. Localization using bidirectional microphones

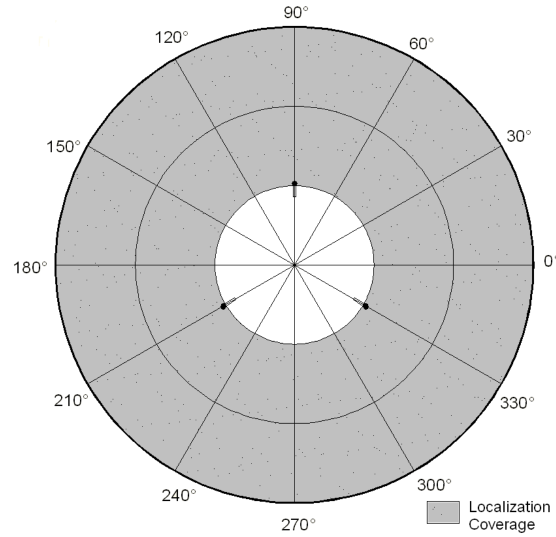

Figure 7(a). Localization sweep using bidirectional microphones

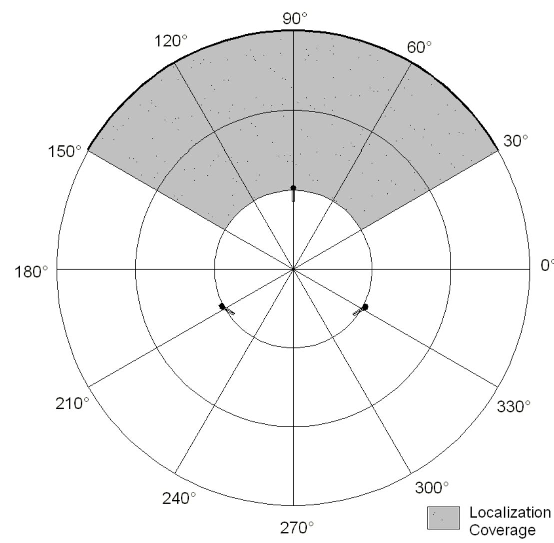

Figure 7(b). Localization sweep using unidirectional microphones

Similar simulations were repeated for the unidirectional microphones arranged at 90°/60°/120° (Figure 7), since the 90°/330°/210° arrangement proved unfeasible due to blind spots (Figure 2).

The plot in Figure 7 shows that the use of three unidirectional microphones provides only 120° coverage. It does not provide full 360° coverage with just three microphones. The proposed method provides complete coverage while keeping the number of microphones low. While the simulation results show the advantages of using the proposed method, experimental results discussed in the next section prove its feasibility.

Experimental Setup

A. Hardware and Software

The experimental setup consisted of three bidirectional microphones, model MXL R144. The manufacturer's frequency response is flat in the range 800-3000Hz. These microphones were connected to an oscilloscope by using XLR to BNC cables. A sound-generation software was developed using visual basic to produce sounds of desired frequencies. The readings taken from the oscilloscope were manually fed into a MATLAB program, which processes the data using the algorithm developed specifically for bidirectional microphones, and points to the location of the sound source with a graph diagram. Each experiment was repeated for 800Hz, 1000Hz and 1200Hz frequencies.

B. Polar Directivity Patterns

Measurements for 360° were taken by rotating the microphones at discrete steps of 10° to find the polar directivity patterns of the microphones. Each microphone was measured for frequencies of 800Hz, 1000Hz and 1200Hz) and, for each frequency, the distances of 6ft., 8ft. and 12ft. between the microphone and SS were considered. The measurements for all three microphones were found to be the same. Figures 8, 9 and 10 show the PDPs obtained from the measured data.

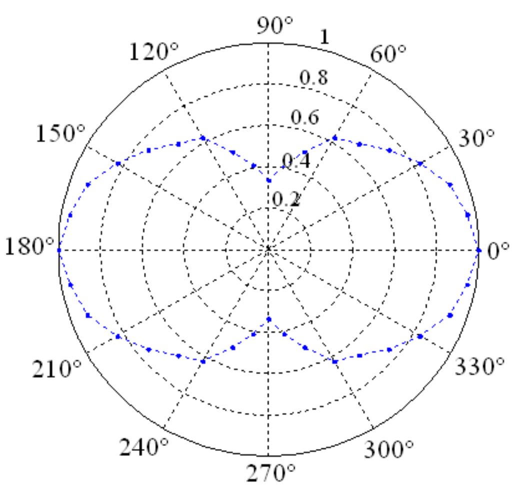

Figure 8(a). PDP at 800Hz and 6 feet from the source

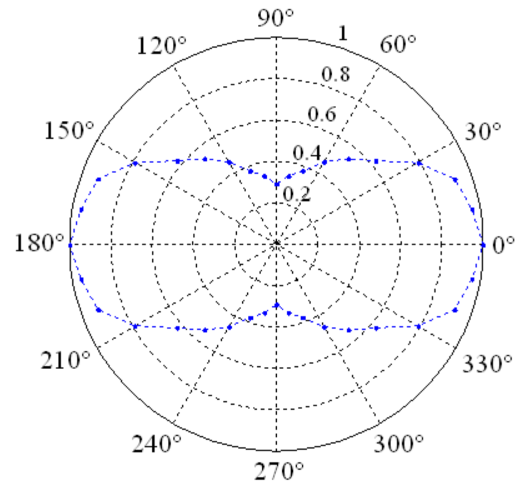

Figure 8(b). PDP at 800Hz and 8 feet from the source

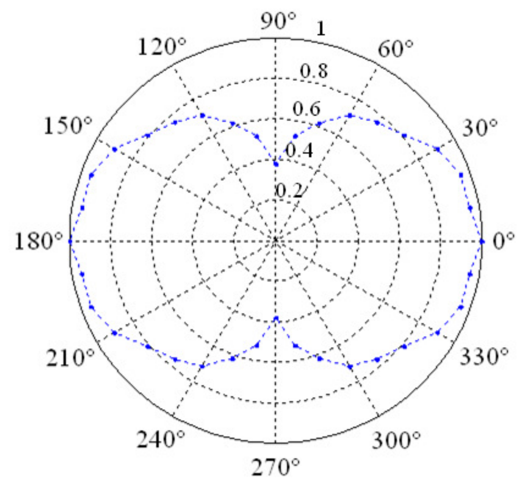

Figure 8(c). PDP at 800Hz and 12 feet from the source

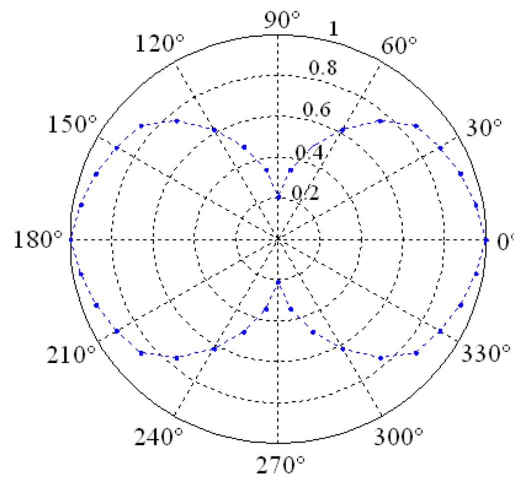

Figure 9(a). PDP at 1000Hz and 6 feet from the source

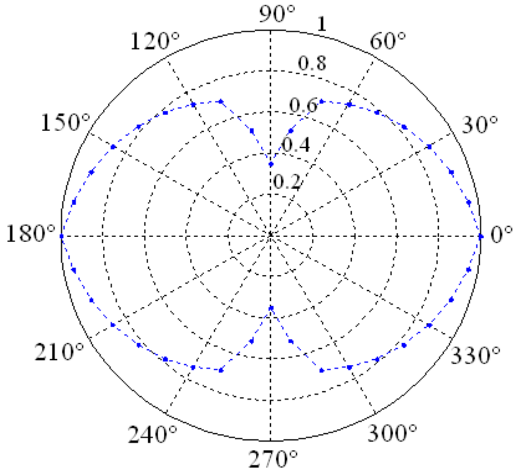

Figure 9(b). PDP at 1000Hz and 8 feet from the source

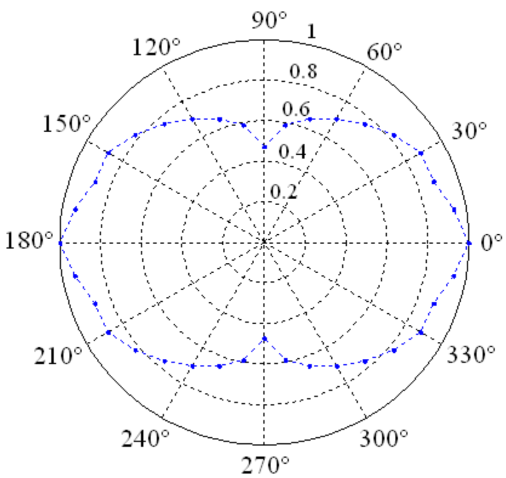

Figure 9(c). PDP at 1000Hz and 12 feet from the source

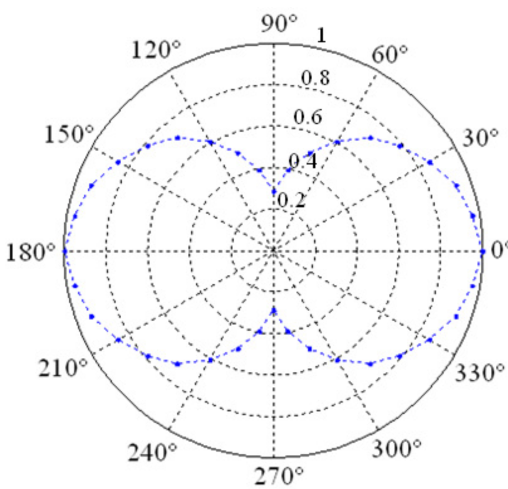

Figure 10(a). PDP at 1200Hz and 6 feet from the source

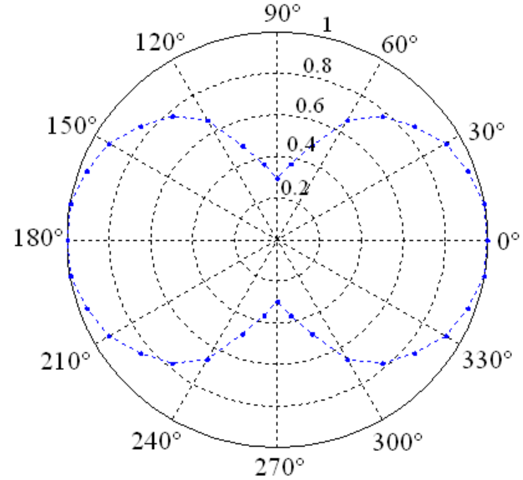

Figure 10(b). PDP at 1200Hz and 8 feet from the source

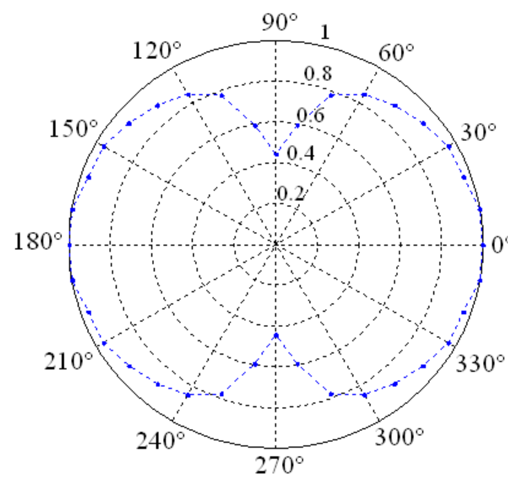

Figure 10(c). PDP at 1200Hz and 12 feet from the source

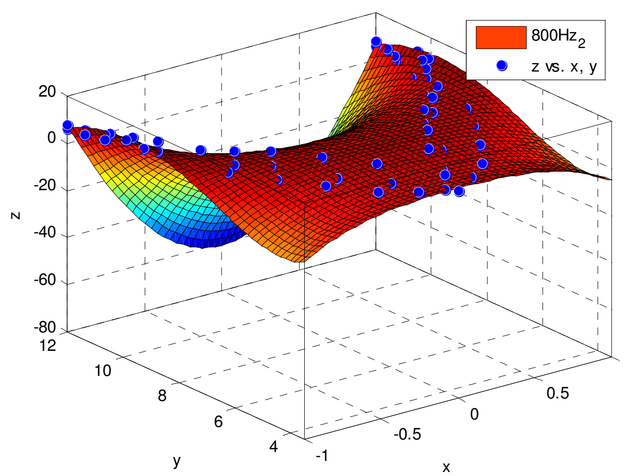

Figure 11. Surface fit using the measured values for 800Hz frequency

Using these results, the aim was to find a fitting equation. By finding the fitting equation, one can generalize it for any distance between the microphone and the SS. To demonstrate this, the surface-fitting toolbox in MATLAB was used. Figure 11 illustrates the surface plot generated for a frequency of 800Hz by taking the data that has been experimentally measured into consideration.

Similar plots for 1000Hz and 1200Hz were generated and the following equations (6), (7), and (8) were obtained for each of the three frequencies (800Hz, 1000Hz, and 1200Hz, respectively).

$$z = 80.18-(46.55)y+(20.14)x^2+(10.34)y^2-(12.94)x^2y \\ -(0.8883)y^3-(6.474)x^4+(1.454)x^2y^2+(0.02239)y^4 \tag{6}$$

$$z = -17.26+(14.95)y+(30.09)x^2-(2.886)y^2-(4.126)x^2y \\ +(0.2208)y^3-(3.434)x^4+(0.1986)x^2y^2-(0.006079)y^4 \tag{7}$$

$$z = -58.73+(38.16)y+(37.61)x^2-(8.161)y^2-(22.98)x^2y \\ +(0.7862)y^3-(48.31)x^4+(1.949)x^2y^2-(0.02798)y^4 \tag{8}$$

With these equations, one can now perform experimental evaluations for various sound-source positions which will be discussed in the next section.

Experimental Results

Equation (1), which was used for simulation earlier, is now replaced with equations (6), (7) and (8) that were extracted from the experimental patterns to localize the SS.

The microphone arrangement was similar to the previous arrangement used for simulation. Here, a few more cases have been considered by decreasing the aperture of the microphone array to show that this method would be useful for making reduced-size sound localizers. First, the microphones were arranged in a circular fashion two feet from the center. Then the distance was reduced to 1 foot and then to 0.5 feet. Each of these arrangements was then tested for three different source locations. The entire process was repeated for the 800Hz, 1000Hz, and 1200Hz frequencies.

Figures 10, 11, and 12 show the experimental results. The three black dots A, B, and C represent the three bidirectional microphones and the red dot O is the origin. The red, green and blue pairs of lines are the directivity lines of the three microphones while the small black squares represent the experimental location of the sound source S_e.

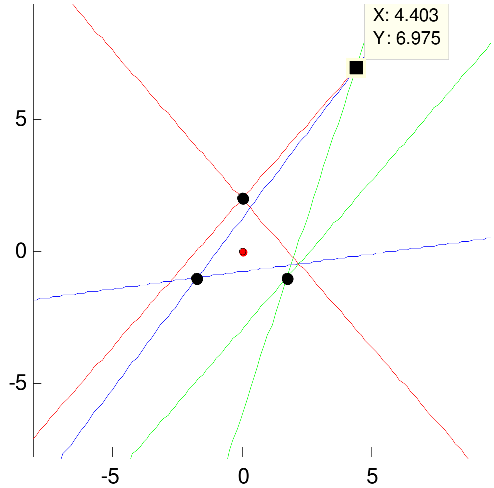

Figure 10(a). Experimental results for Q_{2f} for 800Hz

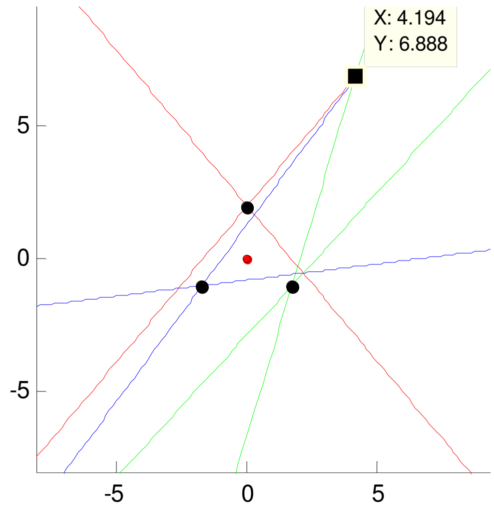

Figure 10(b). Experimental results for Q_{2f} for 1000Hz

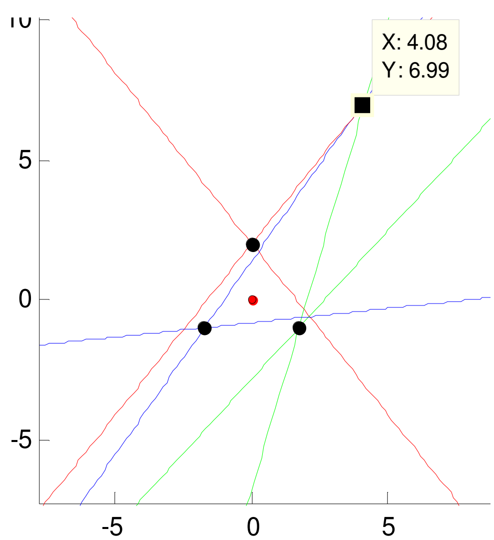

Figure 10(c). Experimental results for Q_{2f} for 1200Hz

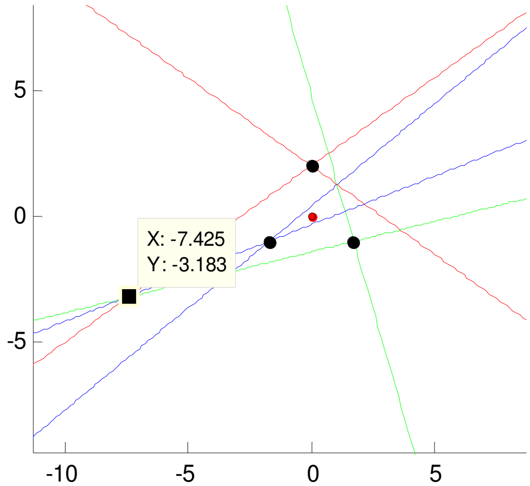

Figure 11(a). Experimental results for R_{2f} for 800Hz

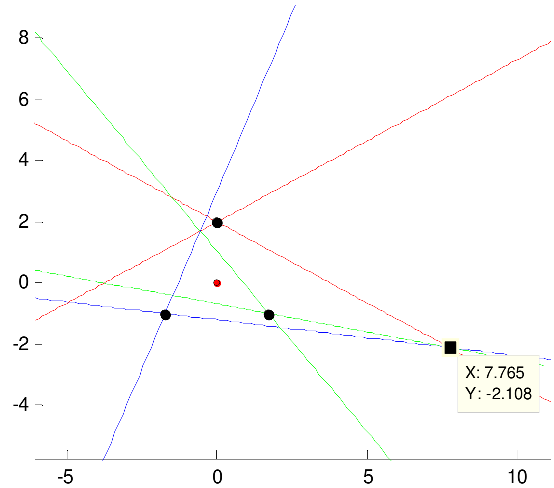

Figure 12(a). Experimental results for S_{2f} for 800Hz

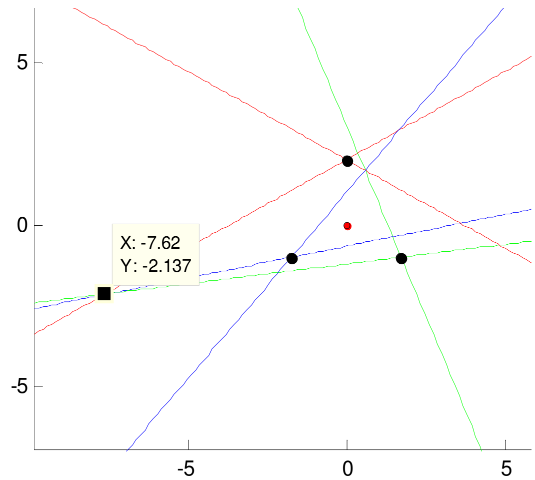

Figure 11(b). Experimental results for R_{2f} for 1000Hz

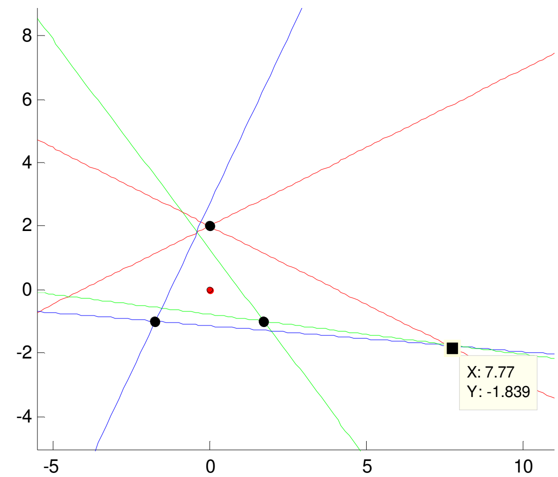

Figure 12(b). Experimental results for S_{2f} for 1000Hz

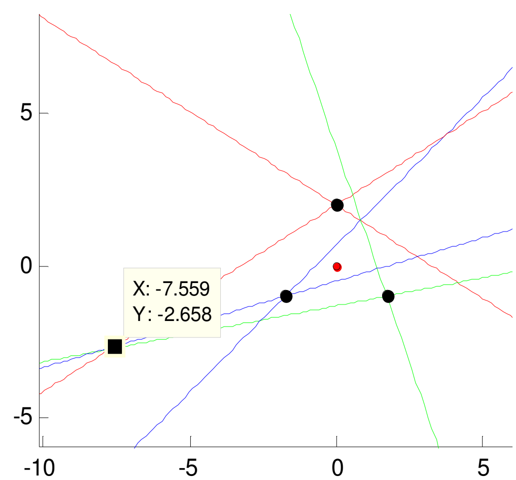

Figure 11(c). Experimental results for R_{2f} for 1200Hz

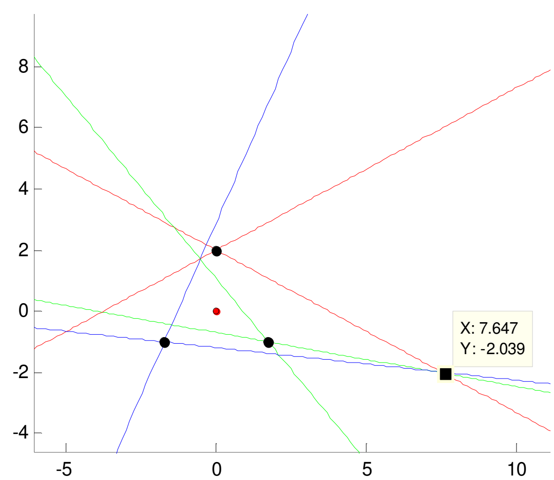

Figure 12(c). Experimental results for S_{2f} for 1200Hz

Table 2. Comparison of experimental results with actual source positions

Source Location	Experimental Location		
	800 Hz	1000 Hz	1200 Hz
Q_{2f}(4.4105,6.8589)	(4.403,6.975)	(4.194,6.888)	(4.08,6.99)
R_{2f}(-7.5473,-2.6339)	(-7.425,-3.183)	(-7.62,-2.137)	(-7.559,-2.658)
S_{2f}(7.0396,2.0503)	(7.765,-2.108)	(7.77,-1.839)	(7.647,-2.039)

Table 2 compares the experimental results obtained for 800 Hz, 1000 Hz, and 1200 Hz frequencies with the actual sound-source location. The above results show that the sound-source positions obtained from the experimental values are very close to the actual positions. The small differences associated with the measured source positions could have resulted from human errors.

The same approach was used to test the reliability of the system by moving the microphones closer. This was tested at distances of 1-foot and 0.5-foot distances from the center to the microphone. The results were similar to the 2-foot arrangement. This shows that the technology is not sensitive to distance.

Certain sound-localization applications in real-life require the sensors to be placed far apart rather than clustering them into a single device. Since the proposed technique employs bidirectional microphones, which are able to “listen” from front and back sides, the “far apart” arrangement is possible, and would require modifications in the proposed algorithm. The current algorithm does not take into account the area between microphones, considering that the aperture is small and it is impractical to have a sound source at that position, i.e. inside the localizing device. If the microphones were to be placed far apart, the area would increase. Accordingly, the algorithm must be revised so that the area gets factored. From yet another perspective, since the aim of the paper is to pave way for miniaturized portable localizers, the aspect of large-aperture testing was not a part of our experiments.

Conclusions

This paper presents a novel sound-source-localization technique based on bidirectional microphones. In contrast to the technique relying on unidirectional microphones, the proposed technique provides complete 360° coverage with no blind spots in the plane of the microphone array. Experiments with different arrangements of microphones and different sound-source positions have been conducted. The sound-source positions have been located by intersecting all possible sound directions identified through the bidirectional polar patterns. The experimental results prove the feasibility of this approach. There was no difference in the results when the microphones were moved closer to each other. It was seen that this technique works for low-aperture microphone arrays, making the system smaller and more portable. This shows that this kind of technology gives rise to a new generation of reduced-size sound localizers. The small differences associated with the measured source location could have been reduced if the microphone and sound source were moved/rotated with a more accurate mechanism instead of using a manual approach.

This study demonstrated the feasibility of the proposed approach which has 360° coverage using just three microphones as opposed to six microphones [1]. Also, this does not have any limitations on the microphone-array aperture like the time-delay approaches.

Future work will involve extending this technique to three-dimensional problems. The possibility of source localization using two microphones could also be evaluated, which could lead to even smaller localizing devices at a reduced cost. The plan is to build a number of hardware prototypes for demonstrating and fine tuning the proposed approach.

Acknowledgements

We gratefully acknowledge Dr. Samir Hefzy (Associate Dean of Graduate Studies and Research Administration, The University of Toledo) for providing financial assistance to Vijay Varada, which made this work possible.

References

[1] P. Rizzo, G. Bordoni, A. Marzani, and J. Vipperman, “Localization of sound sources by means of unidirectional microphones,” Meas. Sci. Technology, 20 055202, 2009.

[2] D. K. Wilson, B. M. Sadler and T. Pham, “Simulation of detection and beamforming with acoustical ground sensors,” Proc. SPIE, Seismic and Acoustic Unattended Ground Sensors I, 2002, vol. 4743, pp. 50–61.

[3] Y. Huang, J. Benesty, and G.W. Elko, “Passive acoustic source localization for video camera steering,” Proc. IEEE Int. Conf. Acoust. Speech Signal Process., 2000, vol. 2, pp. II909-12.

[4] Y. Rui, D. Florencio, W. Lam, and J. Su, “Sound source localization for circular arrays of directional microphones,” Proc. IEEE Int. Conf. Acoust. Speech Signal Process., 2005, vol. 3, pp. 93-6.

[5] M. S. Brandstein and H. F. Silverman, “A practical methodology for speech source localization with microphone arrays,” Comput. Speech Lang, 1997.

[6] J. Benesty, "Adaptive eigenvalue decomposition algorithm for passive acoustic source localization," J. Acoust. Soc. Am., 2000.

[7] S. Bourennane and A. Bendjama, "Locating wide band acoustic sources using higher order statistics," Appl. Acousics, 2002.

[8] G. L. Reid and E. Milios, "Active stereo sound localization," J. Acoust. Soc. Am., 2003.

[9] H. Liu and E. Milios, "Acoustic positioning using multiple microphone arrays," J. Acoust. Soc. Am., 2005.

[10] J. Merimaa, "Application of a 3-D microphone array," Proc. 112th Conv. Audio Eng. Soc., 2002, Paper 5501, pp. 1-10.

[11] X. Bian, G.D. Abowd, and J.M. Rehg, "Using sound source localization in a home environment," Pervasive Comput., 3468, pp. 19-36, 2005.

[12] H. Atmoko, D.C. Tan, G.Y. Tian, and B. Fazenda, "Accurate sound source localization in a reverberant environment using multiple acoustic sensors," Meas. Sci. Technology, vol. 19, 024003, 2008.

[13] B. Kwon, Y. Park and Y-S. Park, "Sound source localization using the compensation method in robot platform," Proc. IEEE Int. Conf. Control Autom. Syst., 2007, pp. 1911–4.

[14] X. Bian, J.M. Rehg, and G.D. Abowd, "Sound Source localization in domestic environment," GVU Center, Georgia Inst. of Technology, 2004.

[15] G. W. Elko, T. C. Chou, R. J. Lustberg and M. M. Goodwin, "A constant-directivity beamforming microphone array (A)," J. Acoust. Soc. Am., 1994.

[16] H-D. Kim, K. Komatani, T. Ogata, and H.G. Okuno, "Design and evaluation of two-channel-based sound source localization over entire azimuth range for moving talkers," Proc. IEEE/RSJ Int. Conf. Intell. Robots Syst., 2008, pp. 2197-2203.

[17] A. Ikeda, H. Mizoguchi, Y. Sasaki, T. Enomoto, and S. Kagami, "2D sound source localization in azimuth and elevation from microphone array by using a directional pattern of element," Proc. IEEE Sensors, 2007, pp. 1213-6.

[18] R. Streincher and W. Doodley, "The bidirectional microphone: a forgotten patriarch," J. Audio Eng. Soc., vol. 51, no. 3, 2003.

Biographies

VIJAY VARADA received the B.Tech. degree in Computer Science from the Jawaharlal Nehru Technological University, Hyderabad, India, in 2008, the M.S. degree in Engineering from the University of Toledo, Toledo, OH, in 2010. He may be reached at vijaykvarada@gmail.com.

HONG WANG received his Ph.D. degree in Computer Science from Kent State University, Kent, OH, in 2006. Currently, he is an Assistant Professor of Computer Science and Engineering Technology at the University of Toledo. His teaching and research interests include Parallel Computing, Bioinformatics, and Embedded System Design. Dr. Wang may be reached at hong.wang2@utoledo.edu.

VIJAY DEVABHAKTUNI received the B.Eng. degree in Electrical and Electronics Engineering and the M.Sc. degree in Physics both from the Birla Institute of Technology and Science, Pilani, Rajasthan, India, in 1996, and the Ph.D. degree in Electronics from the Carleton University, Ottawa, Ontario, Canada, in 2003. Currently, he is an Associate Professor in the EECS Department at the University of Toledo. His research interests include computer aided design (CAD), image/signal processing, modeling, RF/microwave design, optimization and wireless sensing. Dr. Devabhaktuni may be reached at Vijay.Devabhaktuni@utoledo.edu.